BJT Modeling and AC Equivalent Circuit

Basic Concepts:

The key to the transistor small-signal analysis is the use of ac equivalent circuits or models. A model is the combination of circuit elements, properly chosen, that best approximates the actual behavior of a semiconductor device (BJT) under specific operating conditions. Once the ac equivalent circuit has been determined, the graphical symbol of the device can be replaced in the schematic by this circuit and the basic methods of ac circuit analysis (mesh analysis, nodal analysis, and Thevenin's theorem) can be applied to determine the response of the circuit. There are two schools of thought in prominence today regarding the equivalent circuit to be substituted for the transistor: ***hybrid*** and ***r_e model***.

In summary, the ac equivalent circuit of the BJT amplifier is obtained by (see Fig. 12-1):

1. Setting all dc sources to zero and replacing them by a short-circuit equivalent.
2. Replacing all capacitors by a short-circuit equivalent.
3. Removing all elements bypassed by the short-circuit equivalents introduced by stapes 1 and 2.
4. Redrawing the circuit in a more convenient and logical form.
5. Use the ***hybrid*** or r_e equivalent circuit of the BJT to complete the equivalent circuit of the amplifier.
6. Finally, the following parameters are determined for the amplifier:
   a. Input impedance (Z_i). b. Output impedance (Z_o). c. Voltage gain (A_v).
   d. Current gain (A_i). e. Phase relationship (θ).

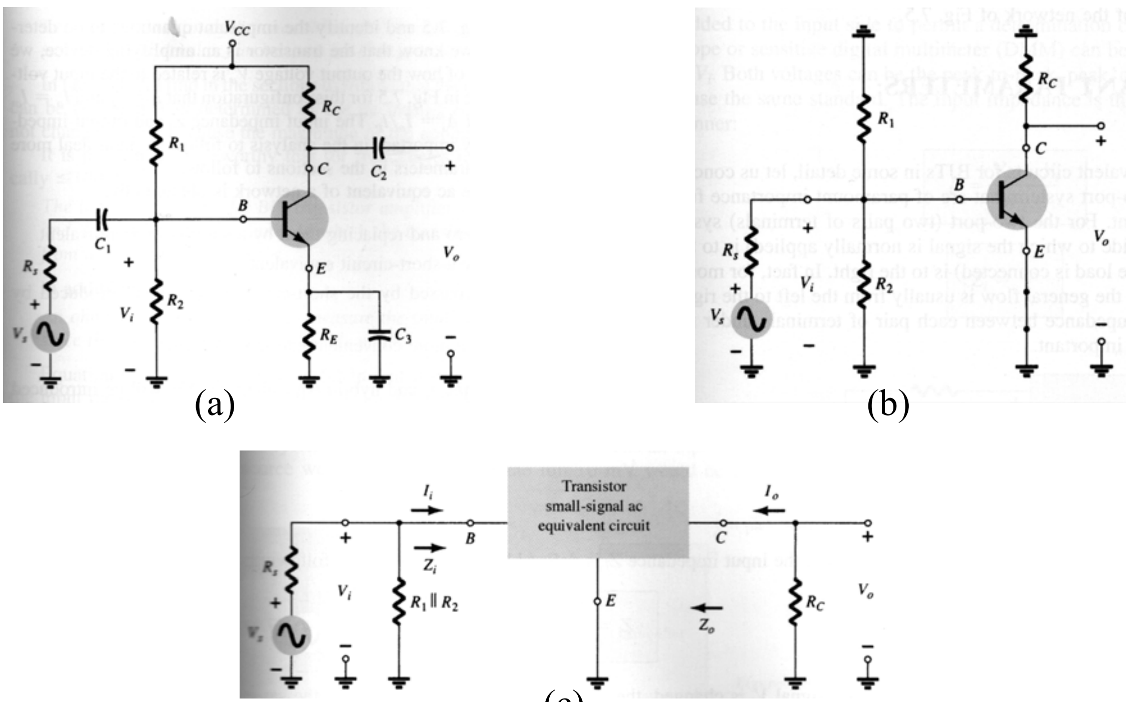

(c)

Fig. 12-1

The Hybrid (h-parameters) Equivalent Model:

For the general hybrid two-port system of Fig. 12-2:

$$V_i = h_{11}I_i + h_{12}V_o \qquad [12.1a]$$
$$I_o = h_{21}I_i + h_{22}V_o \qquad [12.1b]$$

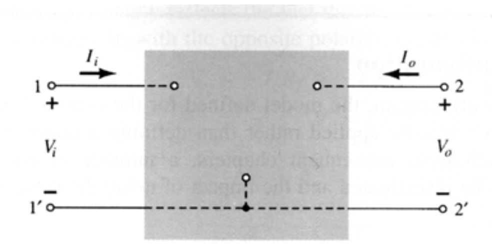

Fig. 12-2

where

$h_{11} = \left.\frac{V_i}{I_i}\right|_{V_o=0} = h_i(\Omega)$, short-circuit input impedance parameter.

$h_{12} = \left.\frac{V_i}{V_o}\right|_{I_i=0} = h_r(unitless)$, open-circuit reverse transfer voltage ratio parameter.

$h_{21} = \left.\frac{I_o}{I_i}\right|_{V_o=0} = h_f(unitless)$, short-circuit forward transfer current ratio parameter.

$h_{22} = \left.\frac{I_o}{V_o}\right|_{I_i=0} = h_o(S)$, open-circuit output admittance parameter.

From the BJT hybrid equivalent circuit of Fig. 12-3, Eqs. [12.1a] and [12.1b] becomes:

$$V_i = h_iI_i + h_rV_o \qquad [12.2a]$$
$$I_o = h_fI_i + h_oV_o \qquad [12.2b]$$

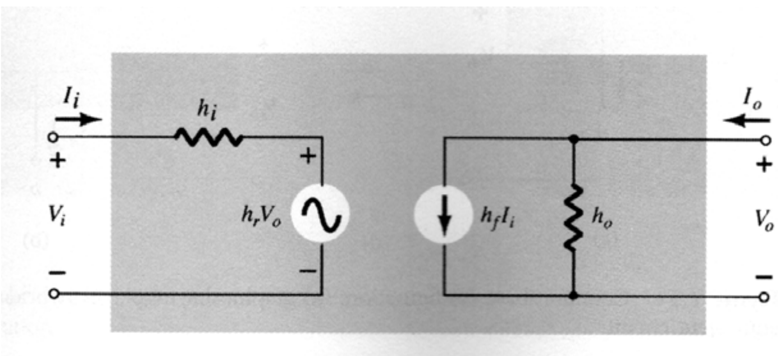

Fig. 12-3

Gain and Impedance Computation of the Complete Hybrid Equivalent Circuit:

For the circuit of Fig. 12-4,

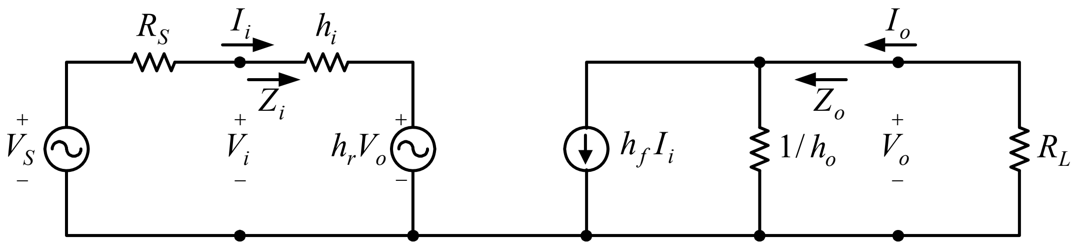

Fig. 12-4

the ***voltage gain*** ($A_v = V_o/V_i$);

$$I_i = \frac{V_i - h_r V_o}{h_i}, \quad I_o = -\frac{V_o}{R_L}, \text{ and } I_o = h_f I_i + h_o V_o \quad \Rightarrow$$

$$\boxed{A_v = \frac{V_o}{V_i} = \frac{-h_f R_L}{h_i + (h_i h_o - h_f h_r) R_L}} \qquad [12.3a]$$

the ***current gain*** ($A_i = I_o/I_i$);

$$I_o = h_f I_i \frac{1/h_o}{1/h_o + R_L} = \frac{h_f I_i}{1 + h_o R_L} \quad \Rightarrow$$

$$\boxed{A_i = \frac{I_o}{I_i} = \frac{h_f}{1 + h_o R_L}} \qquad [12.3b]$$

the ***input impedance*** ($Z_i = V_i/I_i$);

$$\frac{V_i}{I_i} = h_i + h_r \frac{V_o}{I_i}, \text{ and } V_o = -I_o R_L \quad \Rightarrow \quad \frac{V_i}{I_i} = h_i - h_r R_L \frac{I_o}{I_i} = h_i - h_r R_L A_i \quad \Rightarrow$$

$$\boxed{Z_i = \frac{V_i}{I_i} = h_i - \frac{h_f h_r R_L}{1 + h_o R_L}} \qquad [12.3c]$$

the ***output impedance*** ($Z_o = V_o/I_o$ when $V_S = 0$ V);

$$V_S = I_i (R_S + h_i) + h_r V_o = 0 \quad \Rightarrow \quad I_i = -\frac{h_r V_o}{R_S + h_i}, \text{ and } I_o = h_f I_i + h_o V_o \quad \Rightarrow$$

$$I_o = h_o V_o - \frac{h_f h_r}{R_S + h_i} V_o \quad \Rightarrow$$

$$\boxed{Z_o = \frac{V_o}{I_o} = \frac{1}{h_o - \dfrac{h_f h_r}{R_S + h_i}}} \qquad [12.3d]$$

Types of Hybrid Parameters:

Since there are three types of BJT configuration (CE, CC, and CB), there are three different ways that the input and output can be defined and therefore three corresponding sets of *h*-parameters as shown in Table 12-1. If all of the *h*-parameters values in one configuration are known, then the values corresponding to any other configuration can be determined. The common-emitter values of the *h*-parameters are the ones most often given.

Table 12-1

	BJT configuration	*h*-parameters sets
1	Common-Emitter	h_{ie} , h_{fe} , h_{re} , h_{oe}
2	Common-Collector	h_{ic} , h_{fc} , h_{rc} , h_{oc}
3	Common-Base	h_{ib} , h_{fb} , h_{rb} , h_{ob}

The hybrid equivalent circuits of the CE and CB transistor configuration are shown in Fig. 12-5 (a) and (b) respectively.

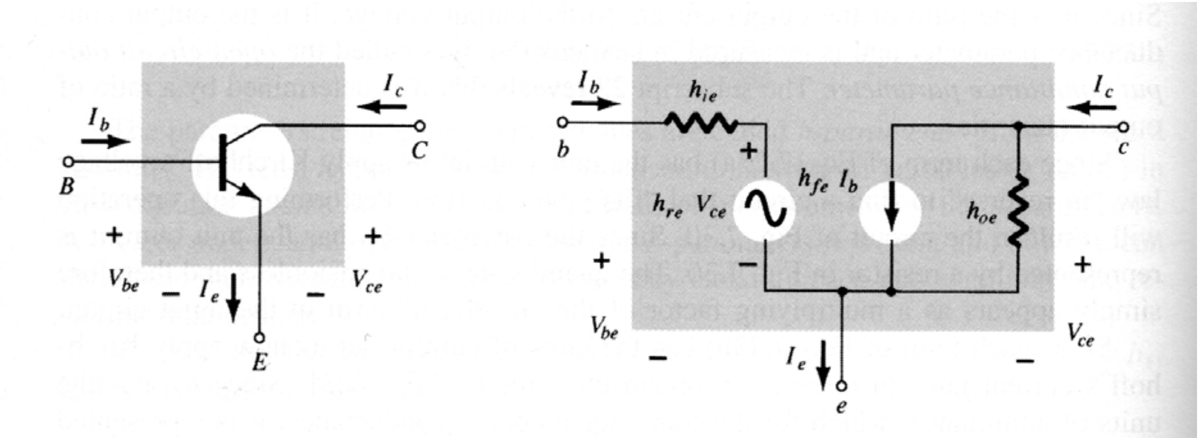

(a)

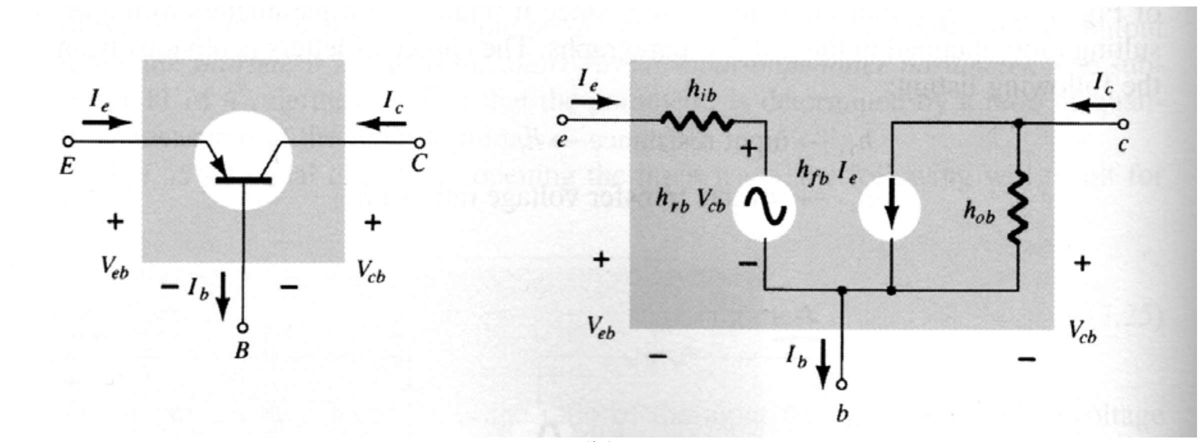

(b)

Fig. 12-5

Table 12-2 lists typical parameter values in each of the three transistor configurations (CE, CC, and CB) for the broad range of transistors available today.

Table 12-2

***h*-parameters**	**CE**	**CC**	**CB**
h_i	1kΩ	1kΩ	20kΩ
h_r	2.5×10^{-4}	≈ 1	3.0×10^{-4}
h_f	50	−50	−0.98
h_o	25 μS	25 μS	0.5 μS
$1/h_o$	40 kΩ	40 kΩ	2 MΩ

Graphical Determination of the CE Hybrid Parameters:

The parameters h_{ie} and h_{re} are determined from the input or base characteristics, while the parameters h_{fe} and h_{oe} are obtained from the output or collector characteristics as shown in Fig. 12-6.

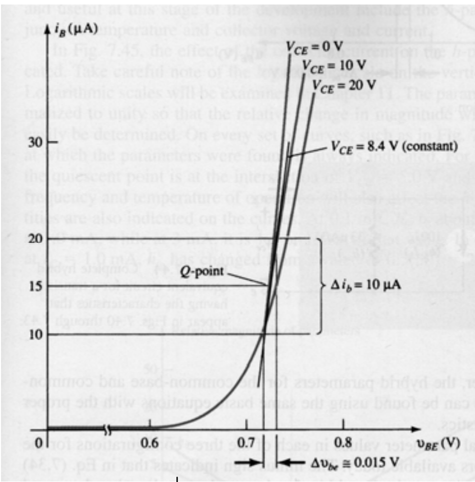

$$h_{ie} = \left.\frac{\Delta v_{be}}{\Delta i_b}\right|_{V_{CE}=const.} = 1.5k\Omega$$

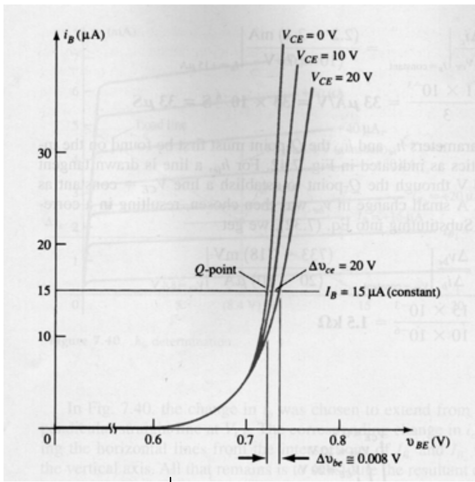

$$h_{re} = \left.\frac{\Delta v_{be}}{\Delta v_{ce}}\right|_{I_B=const.} = 4\times10^{-4}$$

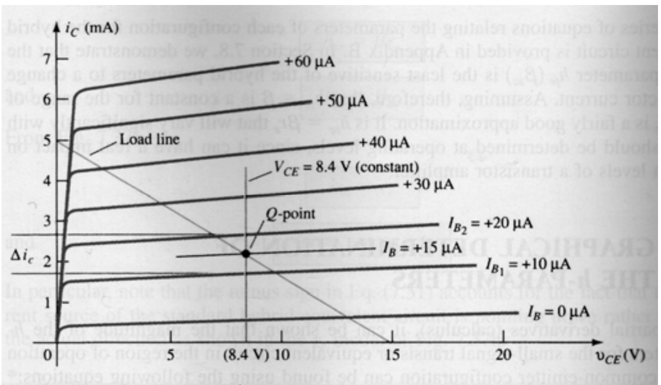

$$h_{fe} = \left.\frac{\Delta i_c}{\Delta i_b}\right|_{V_{CE}=const.} = 100$$

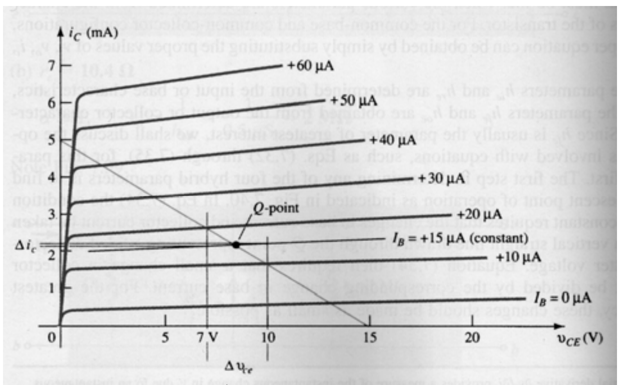

$$h_{oe} = \left.\frac{\Delta i_c}{\Delta v_{ce}}\right|_{I_B=const.} = 33\mu S$$

Fig. 12-6

For the transistor whose characteristics have appeared in Fig. 12-6, the resulting hybrid small-signal equivalent circuit is shown in Fig. 12-7.

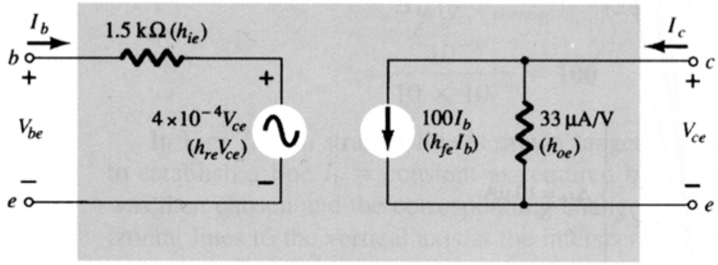

Fig. 12-7

The typical values of h-parameters for CE transistor configuration are shown in Table 12-3.

Table 12-3

h_{xe} parameters		Min.	Max.	Unit
Input impedance	h_{ie}	0.5	7.5	kΩ
Voltage feedback ratio	h_{re}	0.1	8.0	$\times10^{-4}$
Small-signal current gain	h_{fe}	20	250	−
Output admittance	h_{oe}	1.0	30	μS

Approximate CE Hybrid Equivalent Model:

Since h_{re} is normally a relatively small quantity, its removal is approximated by $h_{re} \approx 0$ and $h_{re}V_{ce} = 0$, resulting in a short-circuit equivalent for the feedback element. The resistance determined by $1/h_{oe}$ is often large enough to be ignored in comparison to a parallel load permitting its replacement by an open-circuit equivalent for the CE model as shown in Fig. 12-8.

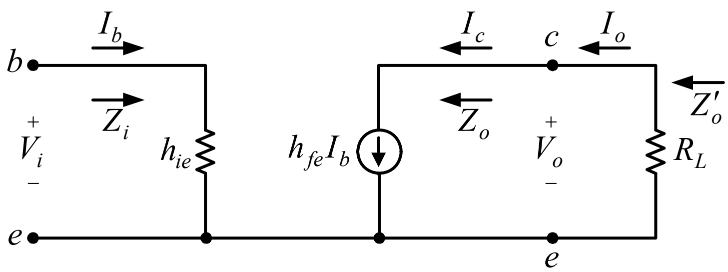

Fig. 12-8

For the circuit of Fig. 12-8,

$$Z_i = h_{ie}, \text{ and } Z_o = \infty .$$

$$A_i = \frac{I_c}{I_b} = h_{fe}, \text{ and } A_v = \frac{V_o}{V_i} = -\frac{I_oR_L}{I_bh_{ie}} = -\frac{I_cR_L}{I_bh_{ie}} = -h_{fe}\frac{R_L}{h_{ie}} = -A_i\frac{Z'_o}{Z_i} .$$

The r_e Equivalent Model:

CB Transistor Configuration:

From Fig. 12-9, the input impedance at the emitter of CB transistor configuration (dynamic resistance of the forward diode) can de determined by:

$$\boxed{r_e = \frac{26mV}{I_E}} \qquad [12.4]$$

the output impedance at the collector (dynamic resistance of the reverse diode) is:

$$\boxed{r_o \approx \infty}$$

also;

$\boxed{Z_i = r_e}$, and $\boxed{Z_o = \infty}$.

$V_o = -I_o R_L = -(-I_c)R_L = \alpha I_e R_L$, and $V_i = I_e Z_i = I_e r_e$ =>

$\boxed{A_v = \frac{V_o}{V_i} = \frac{\alpha R_L}{r_e} \approx \frac{R_L}{r_e}}$.

$I_c = \alpha I_e$, and $A_i = \frac{I_o}{I_i} = -\frac{I_c}{I_e}$ =>

$\boxed{A_i = -\alpha \approx -1}$.

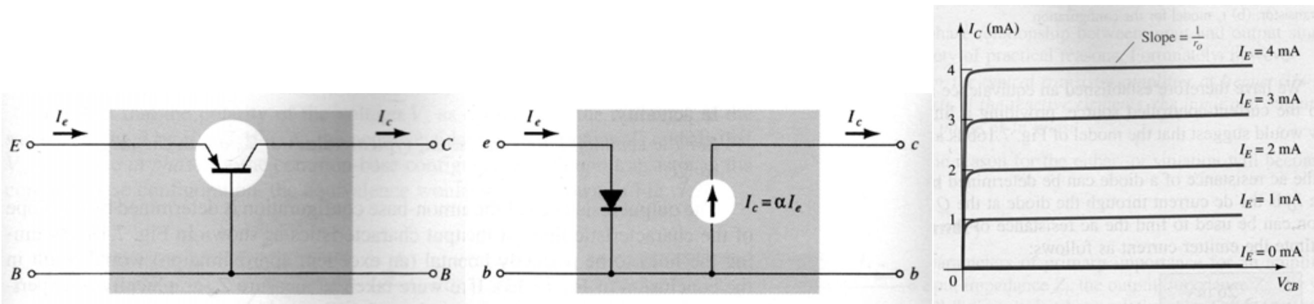

(a) (b) (c)

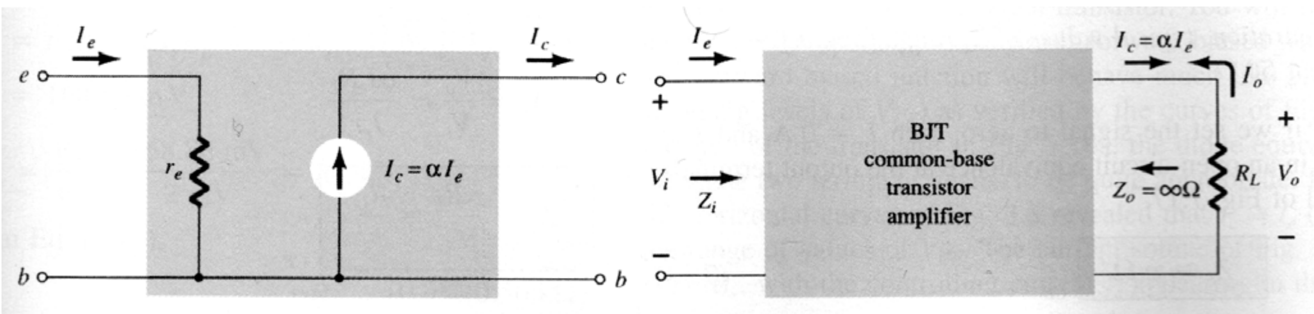

(d) (e)

Fig. 12-9

CE Transistor Configuration:

From Fig. 12-10;

$$I_c = \beta I_b \ , \ \ I_e = I_c + I_b = \beta I_b + I_b = (\beta+1) I_b \approx \beta I_b \ , \quad \text{and}$$

$$V_{be} = I_e r_e \approx \beta I_b r_e \ .$$

$$\boxed{Z_i = \frac{V_i}{I_i} = \frac{V_{be}}{I_b} = \beta \cdot r_e} \ .$$

$$\boxed{Z_o = r_o \approx \infty} \ .$$

$$V_o = -I_o R_L = -I_c R_L = -\beta I_b R_L \, ,$$

$$\boxed{A_v = \frac{V_o}{V_i} = \frac{V_o}{V_{be}} = -\frac{\beta I_b R_L}{\beta I_b r_e} = -\frac{R_L}{r_e}} \ .$$

$$\boxed{A_i = \frac{I_o}{I_i} = \frac{I_c}{I_b} = \frac{\beta I_b}{I_b} = \beta} \ .$$

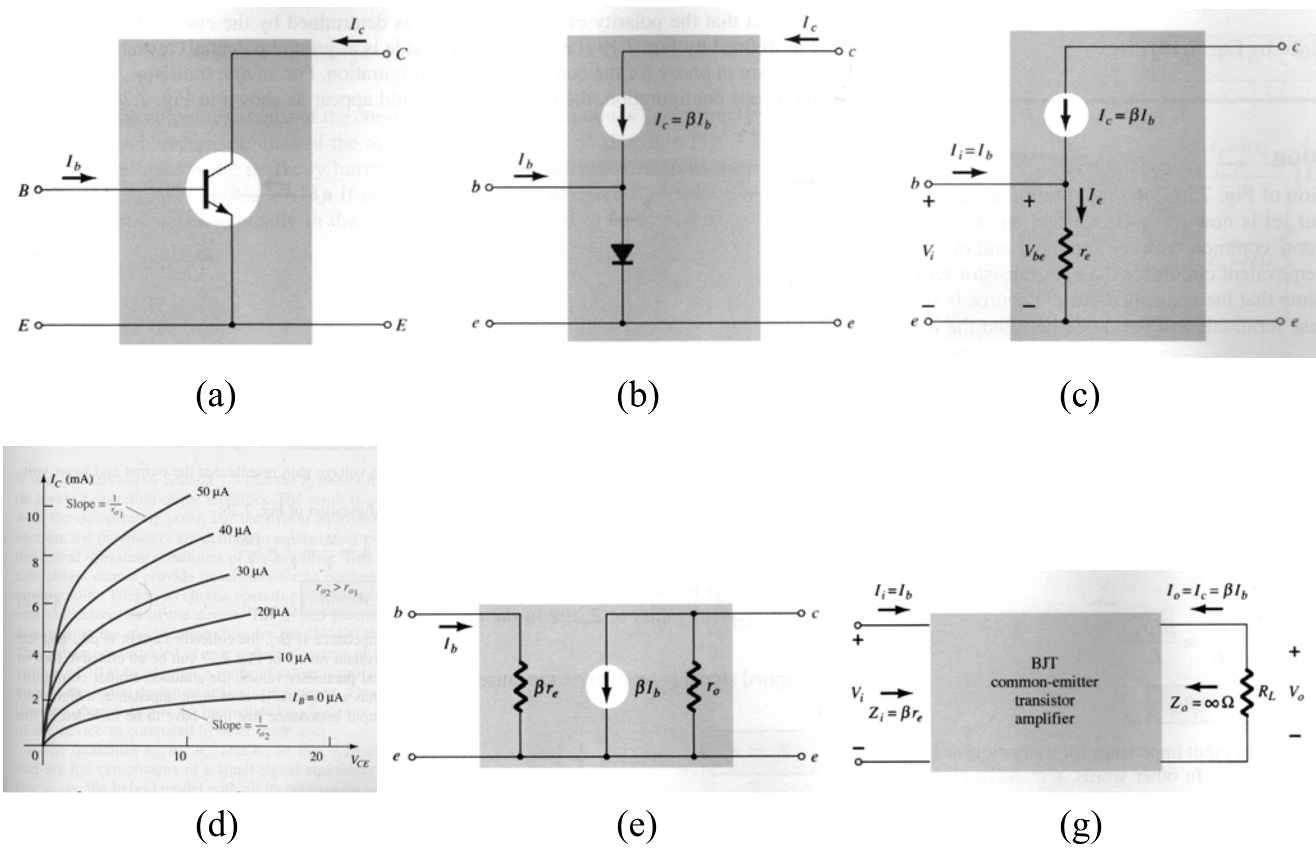

Fig. 12-10